Behavioral/Cognitive

Contributions from Long-Term Memory Explain Superior Visual Working Memory Performance with Meaningful Objects

Hyung-Bum Park[1,2,3] and Edward Awh[1,2]

[1]Institute for Mind and Biology, University of Chicago, Chicago, Illinois 60637, [2]Department of Psychology, University of Chicago, Chicago, Illinois 60637, and [3]Department of Neuroscience, Washington University in St. Louis, St. Louis, Missouri 63110

Working memory (WM) capacity has been claimed to be larger for meaningful objects than for simple features, possibly because richer semantic representations enhance item distinctiveness. However, prior demonstrations compared trial-unique meaningful objects with a small set of repeated simple features. This design confounds meaningfulness with proactive interference (PI), such that PI is minimal for trial-unique objects but substantial for repeated features. Therefore, superior performance for meaningful objects may reflect contributions from episodic long-term memory (LTM) rather than expanded WM capacity. To test this, Experiment 1 measured WM for repeated colors, repeated meaningful objects, and trial-unique meaningful objects from 31 human observers (18 females). The advantage for objects over colors was replicated in the trial-unique condition but eliminated for repeated objects that equated PI across stimulus types. Hierarchical Bayesian dual-process modeling revealed that this advantage reflected stronger familiarity signals, whereas recollection remained stable across stimulus types. Experiment 2 assessed WM storage directly using contralateral delay activity (CDA), an electrophysiological marker of the number of items stored, from 25 observers (14 females). Although trial-unique objects again yielded behavioral advantages, CDA activity across increasing set sizes revealed a common slope and plateau for trial-unique meaningful objects and repeated colors. The CDA difference between stimulus types was additive and did not vary with the set size, providing no evidence for increased WM storage. These findings suggest that object advantages in WM reflect reduced PI and enhanced contributions from LTM. When PI is equated, WM storage limits for simple and meaningful stimuli are equivalent.

Key words: **contralateral delay activity; long-term memory; meaningful objects; proactive interference; working memory capacity**

Significance Statement

Working memory (WM) provides the mental workspace that underlies reasoning, learning, and everyday decision-making, yet its capacity is sharply limited. Previous studies suggested that meaningful, real-world objects are remembered better, raising the possibility that knowledge can expand this known capacity limit. However, many designs confound WM with long-term familiarity. Here, equating proactive interference removed the behavioral advantage for meaningful items. A neural marker of active storage showed additive differences between stimulus types that did not vary with load, indicating no increase in the number of stored items. These findings identify interference, rather than expanded storage, as the source of the reported advantage and offer practical guidance for future experimental design and theories of memory limits.

Introduction

Visual working memory (WM) temporarily maintains information for goal-directed behavior (Cowan, 2001). This online system is limited in capacity to about three items (Luck and Vogel, 1997; Awh et al., 2007; Ngiam et al., 2023; Zhao et al., 2023). Although some models argue against strict item limits (van den Berg et al., 2014; Bays, 2015; Schurgin et al., 2020), broad consensus holds that WM supports a few individuated items with "sufficient fidelity" to guide behavior (Adam et al., 2017; Oberauer and Lin, 2017; Park and Zhang, 2024).

Recent reports of superior WM performance for meaningful objects challenge this fixed-capacity view (Brady et al., 2016; Asp et al., 2021; Torres et al., 2025). Such advantages are often attributed to semantic knowledge that promotes deeper encoding and distinctive representations (Curby et al., 2009; Brady and Alvarez, 2011). However, these demonstrations compared trial-unique objects with a small, repeated set of simple features,

Received Aug. 27, 2025; revised Dec. 10, 2025; accepted Dec. 16, 2025.

Author contributions: H.-B.P. and E.A. designed research; H.-B.P. performed research; H.-B.P. analyzed data; H.-B.P. and E.A. wrote the paper.

This work was supported by the National Institute of Mental Health (ROIMH087214) and Office of Naval Research (N00014-12-1-0972) awarded to E.A.

The authors declare no competing financial interests.

Correspondence should be addressed to Hyung-Bum Park at moonphb@gmail.com.

https://doi.org/10.1523/JNEUROSCI.1660-25.2025

confounding meaningfulness with proactive interference (PI; Kane and Engle, 2000; Jonides and Nee, 2006). With minimal PI for trial-unique stimuli, recognition can rely on global familiarity, producing inflated capacity estimates (Standing, 1973; Endress and Potter, 2014). Thus, meaningful-object benefits may reflect reduced PI and greater contributions from long-term memory (LTM) rather than expanded WM storage.

Prior studies have attempted to control PI using scrambled images that match intact objects in stimulus count and sensory energy (Thibeault et al., 2024). One possibility is that scrambled objects, which lack semantic and categorical distinctiveness, are more confusable with one another; thus the degree to which PI is matched across intact and scrambled conditions remains uncertain. This possibility is consistent with broader PI findings that interference increases when memory items are less distinctive or more confusable (Bunting, 2006; Craig et al., 2013). Repetition frequency should theoretically increase PI (Brady et al., 2025), yet the effect depends on how often items repeat across trials. Consequently, PI differences may still explain previously reported advantages with meaningful objects. Moreover, given extant evidence that WM is less susceptible to PI than LTM retrieval (Oberauer et al., 2017), a PI-driven advantage for meaningful objects would implicate enhanced contributions from LTM rather than an expansion of WM storage.

Neural measures provide complementary tests. Contralateral delay activity (CDA) is a well-established marker tracking the number of items stored in WM (Vogel and Machizawa, 2004; Luria et al., 2016). Larger CDA amplitudes have been reported for meaningful compared with simple stimuli and interpreted as evidence for greater WM storage (Thibeault et al., 2024). However, these studies used only a single set size, obscuring the distinction between increases in WM storage and other load-independent sources of CDA activity. Woodman and Vogel (2008) found that orientations and color-orientation conjunctions elicited larger CDA than colors, but the effect was "additive" with the set size (Fig. 1), indicating stimulus-driven activity rather than an increase in the number of items stored. Similarly, Drew et al. (2011) found larger CDA during multiple-object tracking than static WM tasks, again additive with the set size. These underscore the need to examine CDA across multiple set sizes to identify genuine changes in WM storage. One influential study on meaningfulness benefit did examine multiple set sizes and reported a stimulus-by-set size interaction (Brady et al., 2016), but subsequent work failed to replicate either the neural or behavioral effects (Li et al., 2020; Quirk et al., 2020; but see Thibeault et al., 2024), leaving the robustness of those effects uncertain.

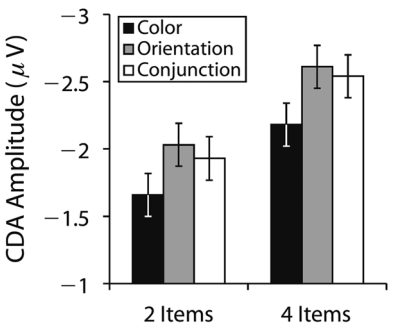

Figure 1. Mean CDA amplitudes for color, orientation, and conjunction stimuli at set sizes 2 and 4, adapted from Woodman and Vogel (2008), their Figure 3*D*. Although orientation and conjunction stimuli elicited larger CDA amplitudes than color stimuli, these differences were additive across set sizes, suggesting that the enhanced CDA was not due to an increased number of items stored in WM.

Here, we examined whether WM could store more meaningful objects than simple features when PI is equated. Experiment 1 compared recognition performance at supra-capacity set sizes across repeated colors, repeated meaningful objects, and trial-unique meaningful objects. Experiment 2 measured CDA across multiple set sizes for repeated colors and unique objects in a lateralized change-detection task. To anticipate, the behavioral advantage for meaningful objects was eliminated under equated PI, and the increase in CDA activity for meaningful objects was additive with the set size, providing no evidence that meaningfulness expands WM capacity.

Materials and Methods

Experiment 1

Participants

Thirty-one volunteers (18 females) participated in the experiments and received monetary compensation ($20 per hour). Participants were aged between 18 and 31 years ($M = 22.3$; SD = 3.2), reported normal or corrected-to-normal visual acuity, and provided informed consent according to procedures approved by the University of Chicago Institutional Review Board.

The sample size was determined via an a priori power analysis (G*Power 3.1; Faul et al., 2009), targeting 85% power to detect a medium effect size (Cohen's $d > 0.5$) in primary comparisons between stimulus conditions at an alpha level of 0.05, based on prior studies investigating visual WM capacity differences between meaningful objects and color stimuli (Brady et al., 2016; Chung et al., 2023, 2024).

Experimental design

Stimuli were generated using MATLAB (The MathWorks) and the Psychophysics toolbox (Brainard, 1997) and presented on an LCD computer screen (BenQ XL2430T; 120 Hz refresh rate; 61 cm screen size in diameter; 1,920 × 1,080 pixels) with a gray background (15.1 cd/m^2) and positioned ~70 cm from participants.

Figure 2 illustrates the stimuli and procedure of the task. Participants performed a visual WM recognition task with a set size of six items across three blocked conditions: trial-repeated colors, trial-repeated meaningful objects, and trial-unique meaningful objects. The block order was counterbalanced across participants. Each block contained 120 trials. Participants were given short breaks between blocks and 20 s breaks after every 40 trials within each block to reduce fatigue.

Each trial started with a 500 ms central fixation cross (0.2° visual angle), followed by a memory array of six items (each 2.0 × 2.0°) presented for 1,000 ms, arranged evenly along an imaginary circle (radius of 5.3°). After a 1,500 ms blank retention interval, participants saw a single central probe, with a semicircular confidence rating scale (radius of 8.2°, thickness of 2.2°) split into left and right sides, separated by 90° gaps and with response regions labeled "NEW" and "OLD," respectively. Participants responded by moving a mouse cursor from the screen center to the continuous scale labeled with discrete confidence markers, "surely new," "probably-new," "guess-new," "guess-old," "probably-old," and "surely old." Probe items were old (presented in the memory array) or new with equal probability.

In both trial-repeated conditions (colors and meaningful objects), memory arrays consisted of six items randomly selected from a fixed set of eight stimuli unique to each condition. The color set consisted of eight categorically distinct hues (RGB values: red [255,0,0], green [0,255,0], blue [0,0,255], magenta [255,0,255], yellow [255,255,0], cyan [0,255,255], orange [255,128,0], and white [255,255,255]). For objects, we selected 964 Microsoft Office icons that were easily recognizable, including animals, plants, foods, transportation, musical instruments, and so forth (see Fig. 2*B* for example stimuli; available at https://osf.io/e8ptm/). These items were presented in black on the gray background. The eight objects in the trial-repeated object condition were randomly sampled from the object pool for each participant

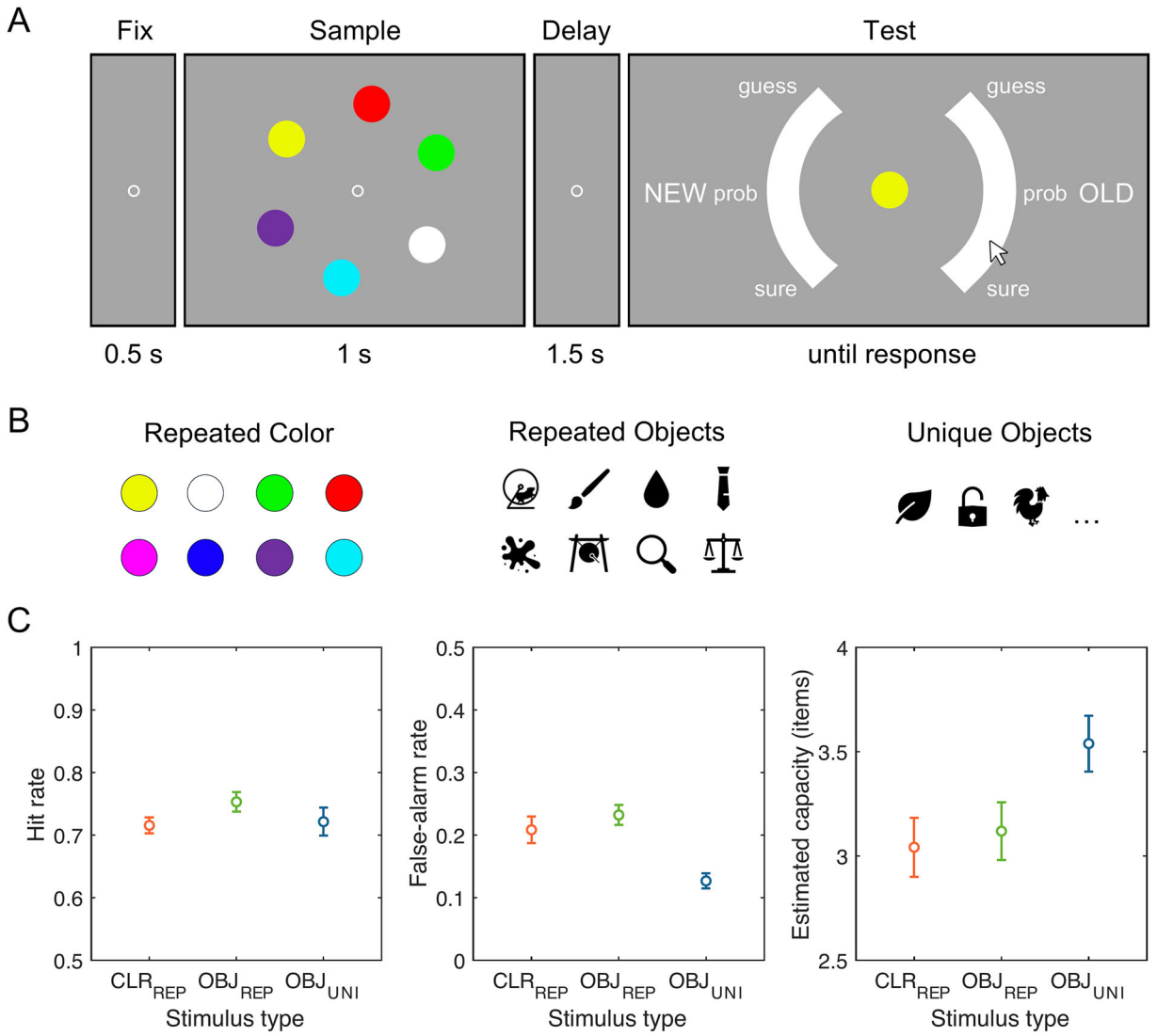

Figure 2. Experimental paradigm and behavioral results from Experiment 1. ***A***, Task sequence for the visual WM recognition task. Each trial began with a fixation display (500 ms), followed by a memory array containing six items (1,000 ms), a blank retention interval (1,500 ms), and a recognition probe requiring a confidence rating on a continuous scale ranging from "sure new" to "sure old." ***B***, Examples of stimulus sets used across three conditions: colors (CLR_{REP}; repeated across trials), meaningful objects repeated throughout the experiment (OBJ_{REP}), and trial-unique meaningful objects presented only once (OBJ_{UNI}). ***C***, Behavioral performance summarized as hit rate (left), false-alarm rate (middle), and estimated visual WM capacity measured by Cowan's *K* (right) for each stimulus condition. Error bars represent standard error of the means.

to minimize potential influence of sampling bias in perceptual or semantic properties. The new probes were selected from the remaining items in the set of eight that were not presented in the current memory array. In contrast, for trial-unique objects condition, six novel objects were randomly selected each trial, with another previously unseen object used as the new probe.

Statistical analysis

Behavioral performance. We calculated hit rates (correctly recognition of old probes) and false alarm rates (incorrect recognition of new probes as old) for each condition. From these, we computed Cowan's *K* (capacity) = set size × (hit rate − false alarm rate).

Hierarchical Bayesian dual-process signal detection modeling. Confidence ratings were derived from the final clicking response along the semicircular response regions and binned into six discrete confidence levels, specifically, three levels of confidence for "old" responses (surely old, probably-old, and guess-old) and three levels for "new" responses (guess-new, probably-new, and surely new). These ratings were used to construct receiver operating characteristic (ROC) curves, plotting cumulative false-alarm rates on the *x*-axis against cumulative and hit rates on the *y*-axis across confidence levels.

These empirical ROCs were fitted with the dual-process signal detection (DPSD) model, which assumes that recognition decisions are based on two independent processes (Yonelinas, 2002; Yonelinas et al., 2010): (1) recollection, which is an all-or-none retrieval of contextual details reflecting context-bound WM representation, and (2) familiarity, which is a continuous signal detection process reflecting context-free episodic LTM traces. The DPSD parameter estimation was performed using a hierarchical Bayesian method, which provides robust population-level estimates of the model parameters by simultaneously accounting for different sources of uncertainty across individual (random) and condition (fixed) effects. The advantage of the hierarchical Bayesian method is especially useful in ROC modeling, wherein a relatively limited number of trials are allocated for each decision criterion (e.g., six-binned confidence level) per experimental condition (Park et al., 2023). The main and interaction effects were estimated in a general linear model, sampled from the normal distribution where the mean is the sum of the fixed and random effects and the variability term is the interaction across effects.

We used Markov chain Monte Carlo sampling to estimate the posterior distributions of the parameters, generating 12,000 samples after 12,000 warm-up iterations. Population-level parameter posteriors were thus represented by a $12{,}000 \times 31 \times 3$ matrix (i.e., samples × participants × stimulus types). We chose noninformative and reasonably informative priors. Model convergence was confirmed by using the Gelman–Rubin diagnostic $\hat{R}$ (Gelman and Rubin, 1992) and found to be close to or equal to 1.0 for all population-level parameters. Figure 3 provides visualization of model fits over empirical ROCs for individual participant. Statistical inference was made based on posterior mean parameter estimates and their associated 95% highest-density intervals ($HDI_{95\%}$). HDIs provide direct estimates of evidence strength, intervals that exclude zero provide strong evidence for credible effects (Kruschke, 2015).

Experiment 2

Participants

Twenty-five volunteers (14 females) participated in Experiment 2. All participants were right-handed, aged 19–32 years ($M = 23.7$; $SD = 3.1$), and reported normal or corrected-to-normal vision. Informed consent was obtained according to procedures approved by the University of Chicago Institutional Review Board. The final sample size of 18 participants and number of trials collected was determined based on prior EEG studies investigating CDA amplitude differences under various stimulus conditions, with an eye toward studies examining the CDA amplitude by set size function (Woodman and Vogel, 2008; Fukuda et al., 2015; Luria et al., 2016). As a consequence, data from seven participants were excluded prior to analysis due to eye movements or EEG artifacts (see below, Artifact rejection, for exclusion criteria).

Experimental design

Participants completed a lateralized change-detection task in two blocked conditions, trial-repeated colors, and trial-unique objects, respectively (Fig. 4*A*). Stimulus generation was identical to Experiment 1. Each trial began with a 500 ms central fixation (radius of 0.2°), followed by a 500 ms arrow cue presented above the fixation circle, indicating the side to remember (left/right, equally probable). A memory array was presented for 1,000 ms. In order to account for the lateralized nature of the CDA component, the memory array contained 1, 3, or 5 items presented in each visual hemifield. For both hemifields, the matching number of items was displayed at randomly chosen locations among five fixed placeholders (3.0 × 3.0° each), two were on an inner imaginary circle of 2.7° radius, and the other three were on an outer imaginary circle of 7.0° radius, with 2.0° lateralized offset from the central midline of the display. After a 1,000 ms retention interval displaying only placeholders, a test probe appeared at one of the remembered item locations on the cued side. Participants indicated whether the probe matched the original item by pressing one of the two buttons, "z" or "/" key to indicate "no-change" or "change," respectively. The probability of change and no-change was equal. Participants completed 200 trials per set size condition in each of the repeated-color and unique-object blocks with a randomized block order across participants.

EEG acquisition

EEG was recorded from 30 active Ag/AgCl electrodes (actiCHamp, Brain Products) mounted in an elastic cap positioned according to the international 10–20 system (Fp1, Fp2, F7, F3, F4, F8, Fz, FC5, FC6, FC1, FC2, C3, C4, Cz, CP5, CP6, CP1, CP2, P7, P8, P3, P4, Pz, PO7, PO8, PO3, PO4, O1, O2, Oz). A ground electrode was placed at position Fpz, and two additional electrodes were affixed with stickers to the left and right mastoids. Data were referenced online to the right mastoid and rereferenced offline to the algebraic average of the left and right mastoids. Incoming data were filtered (low cutoff, 0.01 Hz; high cutoff, 80 Hz; slope from low to high cutoff, 12 dB/octave) and recorded with a 500 Hz sampling rate. Impedance values were kept below 10 kΩ.

Eye movements and blinks were monitored using electrooculogram (EOG) activity and eye tracking. We collected EOG data with five passive electrodes (two vertical VEOG electrodes placed above and below the right eye, two horizontal HEOG electrodes placed ~1 cm from the outer canthi of each eye, and a ground electrode placed on the left cheek). Eye-tracking data were collected using a desk-mounted EyeLink 1000 Plus eye-tracking camera (SR Research) sampling at 1,000 Hz.

Artifact rejection

EEG data were segmented into epochs (−200 to 2,000 ms from memory array onset). An automatic artifact rejection pipeline was applied to detect eye movements, blinks, and EEG artifacts. We implemented a

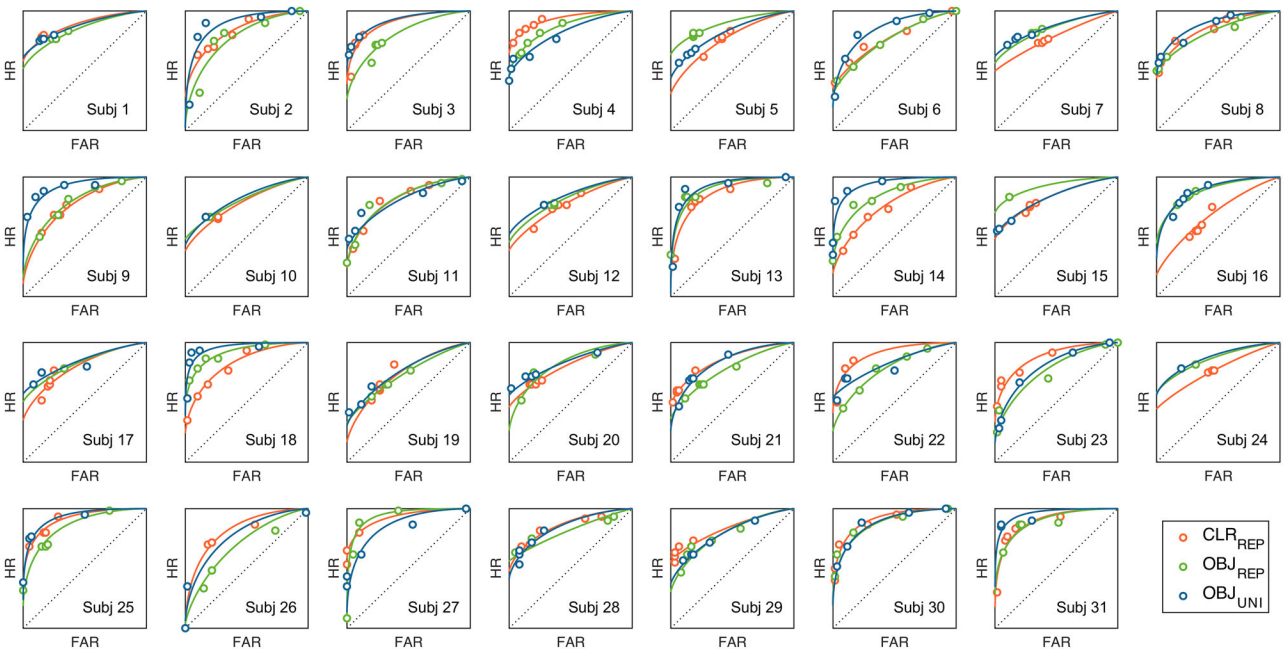

Figure 3. Observed and model-fitted ROC curves for individual participants. Each panel shows hit rate (HR) plotted over false-alarm rate (FAR) across confidence levels from each participant. Solid curves represent model predictions generated by the mean posterior parameters estimated from the hierarchical Bayesian DPSD model. Color codes represented repeated colors (CLR_{REP} in red), repeated objects (OBJ_{REP} in green), and unique objects (OBJ_{UNI} in blue) conditions, respectively. Circles denote observed data. The close correspondence between predicted and observed values indicates good individual-level model fit.

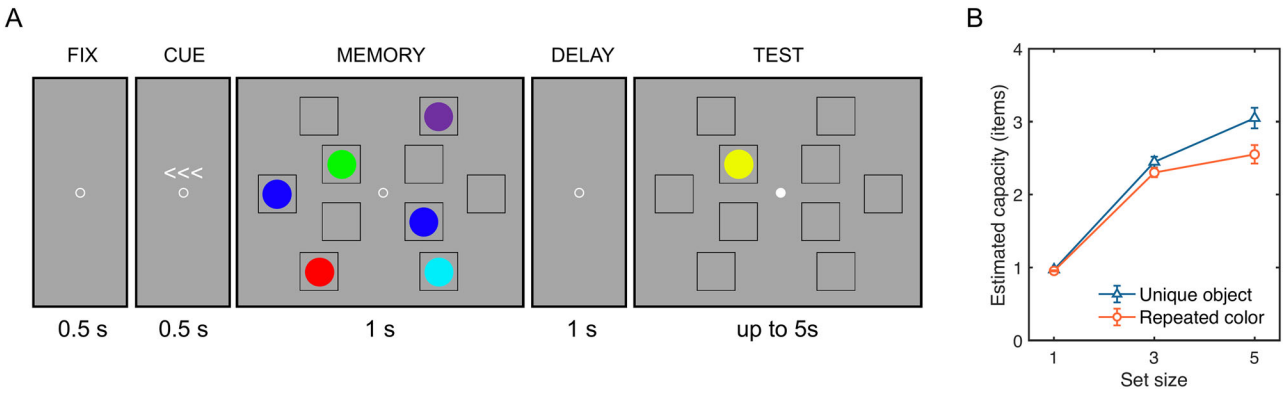

Figure 4. Procedure and resulting capacity estimates for Experiment 2. ***A***, Lateralized visual WM task sequence shown for the color stimulus condition. Each trial began with central fixation (500 ms), followed by an arrow cue indicating the task-relevant hemifield (left or right; 500 ms). The memory array was then presented laterally (1,000 ms), followed by a blank retention interval (1,500 ms). Participants subsequently indicated whether a test probe matched the remembered item at the corresponding location. The fixation point changed its color to white to indicate the onset of test array and allow participants to blink. The trial-unique meaningful object condition used the same procedure, differing only in stimulus content. ***B***, Capacity estimates of mean Cowan's *K*, as a function of set size (1, 3, or 5 items) and stimulus type (unique object vs repeated color). Error bars represent standard error of the mean.

comprehensive set of criteria using ERPLAB functions (Lopez-Calderon and Luck, 2014). Trials contaminated by artifacts were excluded for EEG analyses but not from behavioral analyses. We rejected trials containing eye movements and blinks using EOG channels and eye-tracking data.

For EOG channels, trials were flagged when the absolute voltage exceeded 50 μV or when step-like activity exceeded 30 μV within a 100 ms moving window (advanced in 10 ms steps). For eye-tracking rejection, we applied a similar sliding window to the *x*-gaze coordinates and *y*-gaze coordinates (window size, 100 ms; step size, 10 ms; threshold, 0.5°). When eye-tracking data were not available, we used EOGs to detect saccades and blinks. For EEG artifacts, we checked for drift (e.g., skin potentials) using the *pop_rejtrend* function, excluding trials in which a line fitted to the EEG data had a slope exceeding 75 μV with a minimal R^2 of 0.3. High-frequency noise and muscle artifacts were detected using the *pop_artmwppth* function, excluding trials with peak-to-peak activity >75 μV within a 200 ms sliding window advanced in 100 ms steps. We also excluded trials with absolute voltage exceeding ±100 μV in any EEG channel using the *pop_artextval* function. Additionally, we detected step-like artifacts (which can occur with electrode movement) using the *pop_artstep* function, flagging trials with voltage changes exceeding 60 μV within a 150 ms sliding window advanced in 10 ms steps. For ocular artifacts, we applied separate criteria to EOG channels, using an absolute voltage threshold of ±50 μV and detecting saccade-like step functions exceeding 30 μV within a 100 ms sliding window advanced in 10 ms steps. Trials containing flatline signals were also excluded. Seven participants with rejection rate >30% of trials were excluded from further analysis. Across the remaining participants, an average of 12.7% of trials was rejected, with no significant differences in rejection rates between stimulus conditions or set sizes. CDA was calculated as mean amplitude differences between contralateral and ipsilateral posterior electrodes (PO3/PO4, PO7/PO8, P3/P4, P7/P8; Fig. 5). The average CDA amplitudes were taken from three different measurement windows, during stimulus presentation (i.e., encoding; 400–1,000 ms), delay period (1,400–2,000 ms), and a combined window of 400–2,000 ms following memory onset.

Code availability

All data generated or analyzed during this study are available via the Open Science Framework repository at https://osf.io/e8ptm/.

Results

Experiment 1

Experiment 1 tested whether superior visual WM performance for meaningful objects reflects enhanced WM capacity or reduced PI. Recognition performance was compared across repeated colors, repeated objects, and trial-unique objects. If meaningfulness genuinely expands WM capacity, the object advantage should persist regardless of stimulus repetition. Conversely, if the benefit arises from the absence of PI in trial-unique stimuli, the advantage should disappear for repeated meaningful objects that equate PI.

Behavioral performance

Figure 2*C* summarizes the hit rates, false alarm rates, and Cowan's *K* values across the three experimental conditions. First, a one-way repeated–measure analysis of variance (ANOVA) on the mean Cowan's *K*s revealed a significant main effect of stimulus type ($F_{(2,90)} = 3.74$; $p = 0.028$; $\eta_p^2 = 0.08$). This effect was found to be primarily driven by higher capacity estimates for trial-unique objects ($M = 3.54$; SD = 0.75) compared with both trial-repeated colors ($M = 3.04$; SD = 0.79) and trial-repeated objects ($M = 3.12$; SD = 0.77; $ts_{(30)} > 2.69$; Bonferroni-corrected $ps_{bonf} < 0.036$; $ds > 0.49$). Critically, Cowan's *K* estimates did not significantly differ between trial-repeated colors and trial-repeated objects ($t_{(30)} = -0.42$; $p_{bonf} = 1.000$; $d = -0.08$).

Further analysis of hit and false alarm rates revealed that the observed advantage for trial-unique objects primarily stemmed from its reduced false alarms rather than enhanced hit rates. Specifically, for hit rates, a one-way repeated–measures ANOVA indicated no significant effect of stimulus type ($F_{(2,90)} = 1.36$; $p = 0.263$; $\eta_p^2 = 0.03$), with highly comparable performance for trial-repeated colors ($M = 0.72$; SD = 0.07), trial-repeated objects ($M = 0.75$; SD = 0.09), and trial-unique objects ($M = 0.72$; SD = 0.13; $ts_{(30)} < 1.93$; $ps_{bonf} > 0.188$; $ds < 0.35$). In contrast, false alarm rates varied significantly by the stimulus type ($F_{(2,90)} = 10.61$; $p < 0.001$; $\eta_p^2 = 0.19$), with trial-unique objects showing substantially fewer false alarms ($M = 0.13$; SD = 0.07) compared with both trial-repeated colors ($M = 0.21$; SD = 0.12) and trial-repeated objects ($M = 0.22$; SD = 0.09; $ts_{(30)} > 3.85$; $ps_{bonf} < 0.002$; $ds > 0.70$). False alarm rates did not differ significantly between trial-repeated colors and trial-repeated objects ($t_{(30)} = 1.06$; $p_{bonf} = 0.889$; $d = 0.19$).

DPSD modeling

The hierarchical Bayesian DPSD model revealed a clear dissociation between recollection and familiarity processes across stimulus types (Fig. 6). Recollection estimates were highly comparable across all three conditions, with substantial overlaps in their posterior distributions between trial-repeated colors ($M = 0.35$;

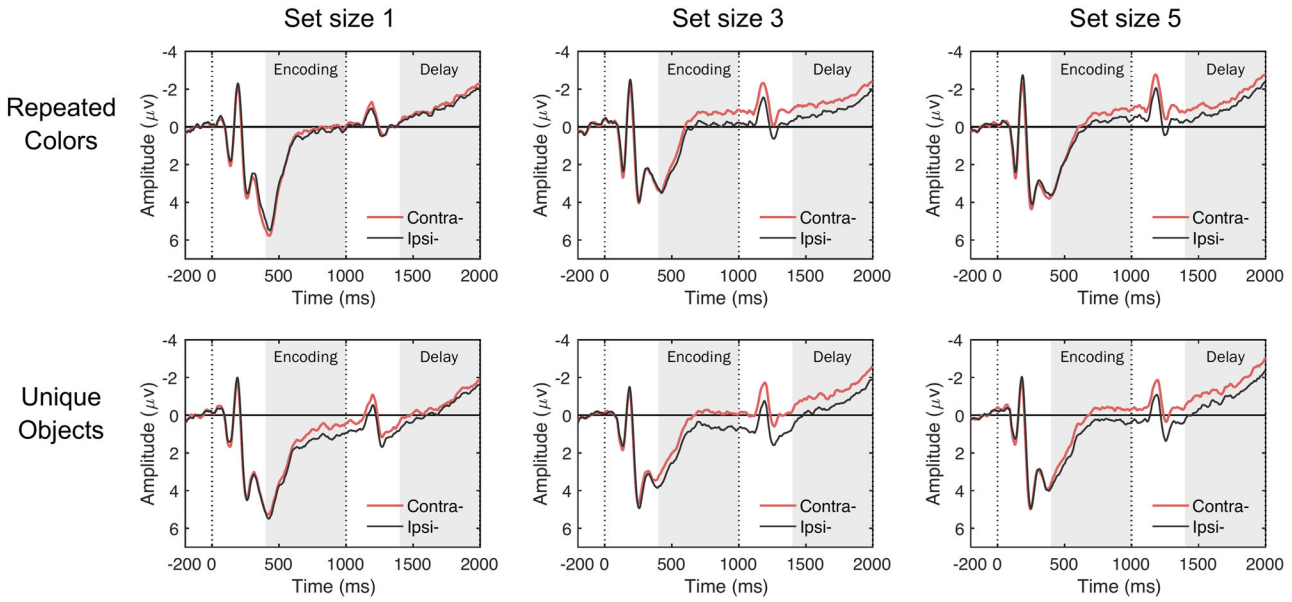

Figure 5. Grand-averaged contralateral and ipsilateral waveforms by the stimulus type and set size. Waveforms are time-locked to the memory array onset (0 ms) and offset (1,000 ms) and averaged across posterior electrode sites (P3/P4, P7/P8, PO3/PO4, PO7/PO8) in Experiment 2. Each panel compares contralateral (red) and ipsilateral (black) activity for trial-repeated colors (top row) versus trial-unique objects (bottom row) at set sizes 1, 3, and 5 (left to right). Vertical dotted lines mark the onset and offset of the memory array.

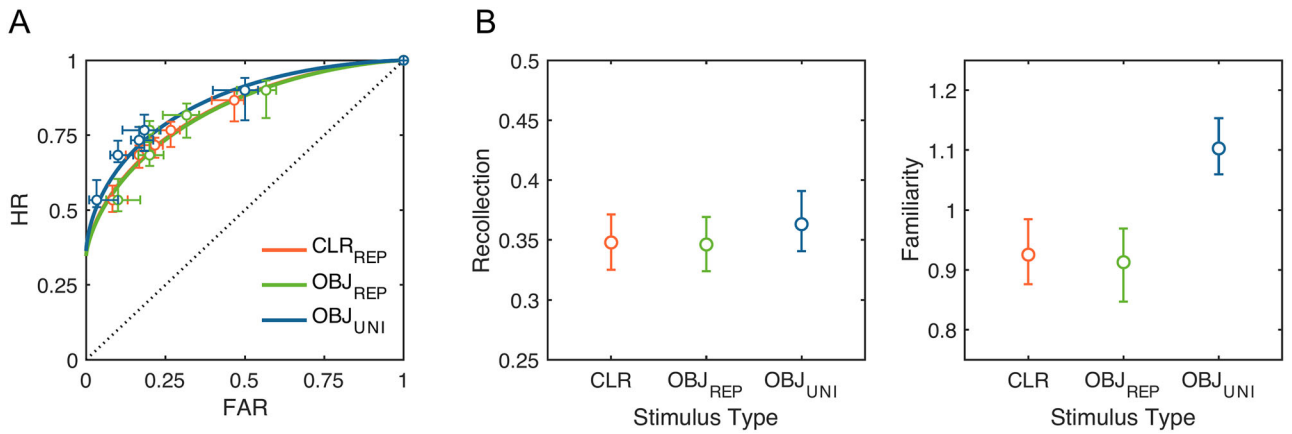

Figure 6. Observed and model-predicted ROC curves and posterior parameter estimates from the hierarchical Bayesian DPSD model. ***A***, ROC curves for each stimulus condition: repeated colors (CLR_{REP}; red), repeated meaningful objects (OBJ_{REP}; green), and trial-unique meaningful objects (OBJ_{UNI}; blue). Circles represent observed mean hit rates (HR) and false-alarm rates (FAR) across confidence levels, and the horizontal and vertical error bars indicate standard errors of the mean FAR and HR, respectively. Solid lines depict model-predicted ROC curves based on posterior mean values of the model parameters. ***B***, Posterior means and $HDIs_{95\%}$ for the population-level recollection (left) and familiarity (right) parameters, across stimulus types. The boundaries of $HDI_{95\%}$ not crossing over between conditions indicate a statistically credible difference.

$HDI_{95\%}$ [0.33, 0.37]), trial-repeated objects ($M = 0.35$; $HDI_{95\%}$ [0.32, 0.37]), and trial-unique objects ($M = 0.36$; $HDI_{95\%}$ [0.34, 0.39]). In contrast, familiarity estimates exhibited a robust effect consistent with the results of Cowan's *K*. Familiarity was credibly higher for trial-unique objects ($M = 1.10$; $HDI_{95\%}$ [1.06, 1.15]) compared with both trial-repeated colors ($M = 0.93$; $HDI_{95\%}$ [0.88, 0.98]) and trial-repeated objects ($M = 0.91$; $HDI_{95\%}$ [0.85, 0.97]), with nonoverlapping credible intervals providing strong evidence for this difference.

Together, these behavioral modeling results show that the object advantage reflected reduced PI with trial-unique stimuli rather than increased WM capacity. As in prior work, this advantage emerged only with trial-unique items (Endress and Potter, 2014) and disappeared when PI susceptibility was equated via repeated presentations. Further analyses indicated that the trial-unique benefit was driven by reduced false alarms, consistent with lower PI rather than enhanced hit rates. Hierarchical DPSD modeling revealed comparable recollection estimates, interpreted as indices of context-bound WM representations, across stimulus conditions, whereas familiarity-based signals were selectively elevated for trial-unique meaningful objects. Consistent with dual-process accounts in which both recollection and familiarity can draw on LTM (Yonelinas, 2024), this pattern does not imply a strict mapping of familiarity to LTM and recollection to WM. Nevertheless, because WM storage is generally less vulnerable to PI than LTM retrieval (Cowan, 2005; Oberauer et al., 2017), the elimination of the meaningfulness advantage under PI aligns with a shift in LTM contributions rather than enhanced WM storage. Notably, this pattern contrasts with reports that real-world objects can increase both recollection and familiarity (compared

with scrambled objects) when low-level properties and repetition statistics are controlled (Torres et al., 2025). Although those findings demonstrate robust effects of meaningfulness on memory performance, they do not determine whether the advantage reflects enhanced WM storage or greater LTM support. Given clear evidence that LTM performance is improved with meaningful stimuli (Shoval et al., 2023), there remains strong motivation for studies that can more conclusively dissociate online storage in WM and enhanced retrieval from LTM.

Experiment 2

Experiment 1 suggested that the meaningful object advantage is most consistent with reduced PI and enhanced contributions from LTM rather than expanded WM capacity. Experiment 2 provided a complementary test using CDA, a neural marker of active WM storage, in a lateralized change-detection task for trial-repeated colors and trial-unique meaningful objects across varying set sizes (1, 3, or 5 items). The critical test concerns the "interaction" between the set size and stimulus type (Fig. 7). If meaningful objects increase visual WM capacity, CDA amplitude should rise with the set size and plateau at a higher level for meaningful objects than for simple features, producing a significant set size × stimulus type interaction. Alternatively, if the advantage reflects contributions from episodic familiarity under PI-free conditions, no change in the shape of the CDA by set size function is predicted.

Behavioral performance

Behavioral results mirrored those of Experiment 1 (Fig. 4*B*). A two-way repeated–measure ANOVA on Cowan's *K* as a function of the stimulus type (trial-repeated color vs trial-unique object) and set size (1, 3, vs 5 items) revealed significant main effects of the stimulus type ($F_{(1,24)} = 13.61$; $p = 0.001$; $\eta_p^2 = 0.36$) and set size ($F_{(2,48)} = 46.28$; $p < 0.001$; $\eta_p^2 = 0.91$). The set size × stimulus type interaction effect was also significant ($F_{(2,48)} = 12.76$; $p < 0.001$; $\eta_p^2 = 0.35$). Notably, the interaction effect was primarily driven by a significant difference in the *K* estimate at set size 5, with trial-unique objects being higher capacity estimates ($M = 3.05$; SD = 0.70) compared with trial-repeated colors ($M = 2.55$; SD = 0.63; $t_{(24)} = 4.04$; $p_{bonf} = 0.001$; $d = 0.82$). The difference in the *K* estimates between the stimulus type at set size 1 (for unique objects, $M = 0.97$; SD = 0.04; for repeated colors, $M = 0.95$; SD = 0.04) and set size 3 (for unique objects, $M = 2.45$; SD = 0.37; for repeated colors, $M = 2.30$; SD = 0.33) did not yield statistical significance ($ts_{(24)} < 2.45$; $ps_{bonf} > 0.066$; $d < 0.50$). Thus, we obtained another clear replication of the behavioral advantage for trial-unique meaningful objects and simple colors. This puts us in a strong position to use CDA activity to determine whether this behavioral advantage is due to increasing online storage in WM rather than enhanced contributions from LTM that would not yield an interaction between CDA activity and set size.

CDA results

Figure 8 shows the grand-averaged CDA waveforms and mean amplitudes across different time windows. In the combined analysis window (Fig. 8*B*, right), a two-way repeated–measure ANOVA with factors of the stimulus type (trial-repeated color vs trial-unique object) and set size (1, 3, 5 items) revealed significant main effects of stimulus type ($F_{(1,17)} = 21.33$; $p < 0.001$; $\eta_p^2 = 0.56$) and set size ($F_{(2,34)} = 19.42$; $p < 0.001$; $\eta_p^2 = 0.53$). Critically, the set size × stimulus type interaction was not significant ($F_{(2,34)} = 0.28$; $p = 0.760$; $\eta_p^2 = 0.02$), indicating that although meaningful objects elicited larger CDA amplitudes overall, this effect was "additive" with the set size, indicating that it reflected a "stimulus-driven" increase in contralateral negativity that was independent of the number of items stored in WM.

These results patterns remained the same when analyzing the separate time windows during stimulus presentation (i.e., encoding; Fig. 8*B*, left) or delay period (i.e., delay; Fig. 8*B*, middle), both showing that the two-way interaction effects did not achieve statistical significance [$F_{(2,34)} = 1.44$; $p = 0.250$, $\eta_p^2 = 0.08$ (encoding) and $F_{(2,34)} = 0.01$; $p = 0.909$; $\eta_p^2 = 0.01$ (delay)]. Furthermore, including measurement window as a factor (encoding vs delay) in a three-way ANOVA revealed no significant main effect of window ($F_{(1,17)} = 0.17$; $p = 0.682$; $\eta_p^2 = 0.01$) nor a three-way interaction ($F_{(2,34)} = 0.171$; $p = 0.843$; $\eta_p^2 = 0.01$); these findings demonstrate that while meaningful objects elicited larger CDA amplitudes than colored squares, the effect was purely additive and did not reflect an increase in active storage capacity.

Taken together, Experiment 2 yielded a clear dissociation between behavioral and the neural signature of active storage.

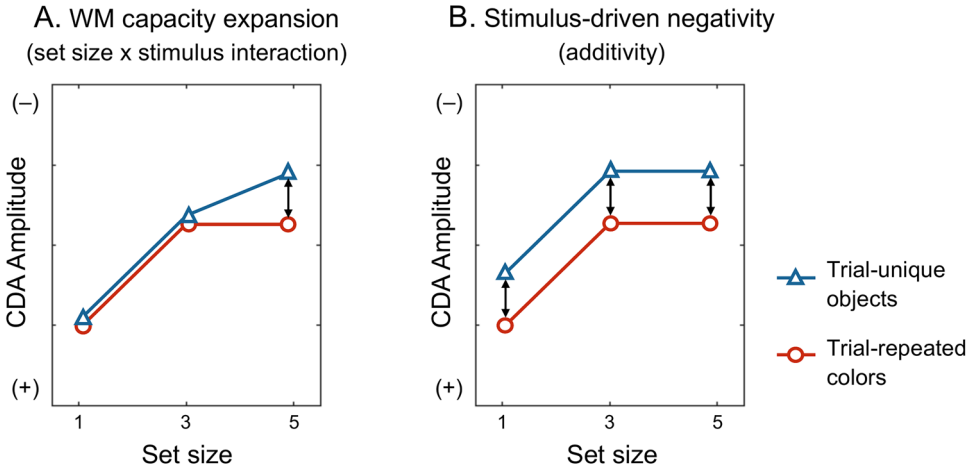

Figure 7. Hypothetical CDA amplitude patterns predicted by competing hypotheses. ***A***, If remembering meaningful objects truly expands visual WM capacity, the CDA amplitude should exhibit a significant set size × stimulus type interaction effect, with CDA amplitude increasing across a larger range of set sizes (set size 5). ***B***, In contrast, a stimulus-related confound hypothesis predicts only additive amplitude differences between stimulus types across all set sizes, without interaction.

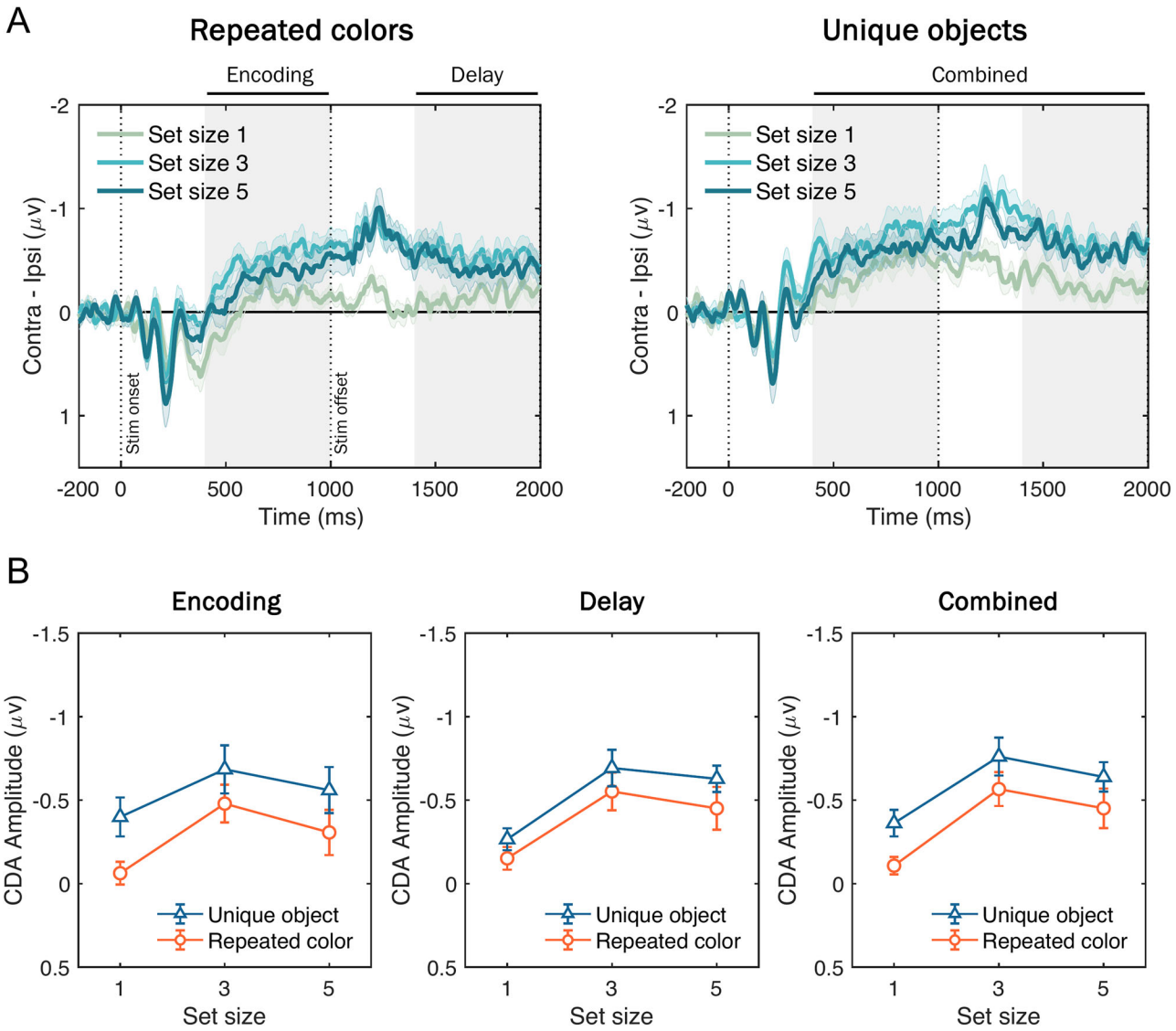

Figure 8. Grand-averaged CDA waveforms and mean amplitudes for trial-repeated colors and trial-unique objects. ***A***, CDA activity (contralateral minus ipsilateral activity at posterior electrode sites; P3/P4, P7/P8, PO3/PO4, PO7/PO8) time-locked to the memory onset and averaged across participants, plotted separately for repeated colors (left) and unique objects (right) at set sizes 1 (green), 3 (sky blue), and 5 (blue). Vertical dotted lines mark stimulus onset (0 ms) and offset (1,000 ms), and gray shading indicates encoding (400–1,000 ms from stimulus onset), delay (1,400–2,000 ms), and combined (400–2,000 ms) measurement windows. Shaded error bars indicate standard error of the means (SEM). ***B***, Mean CDA amplitudes during the early (left), late (middle), and combined (right) time windows as a function of set size for unique objects (triangles on blue line) versus repeated colors (circles on red line). Error bars indicate SEM.

Although behavioral data showed superior performance for trial-unique meaningful objects over repeated colors, the shape of the CDA by set size function revealed that the same number of items were stored in WM. If subjects were able to store more meaningful objects than simple colors, the difference in CDA amplitudes should have been larger for set size 5 where the clearest behavioral benefits were observed for meaningful objects over repeated colors. Instead, CDA differences between meaningful and simple objects were equivalent across all set sizes, suggesting a stimulus-driven contralateral negativity that is independent of the number of items stored in WM (Woodman and Vogel, 2008; Drew et al., 2011). Thus, online neural measures of WM storage disconfirm the hypothesis that WM capacity is expanded for meaningful objects.

Discussion

The present study provides behavioral and neural evidence that question claims that WM capacity can be expanded for meaningful objects compared with simple features. In Experiment 1, meaningfulness and PI were manipulated independently. The performance advantage for meaningful stimuli was driven by trial-unique stimulus presentations that minimized PI rather than by meaningfulness itself. When PI was equated through stimulus repetition, capacity estimates for meaningful and simple stimuli converged. Hierarchical Bayesian DPSD modeling further revealed that the trial-unique advantage was selectively expressed in the familiarity parameter, whereas recollection-based WM processes, maintained by attentional pointers that bind perceptual content to spatiotemporal context (Awh and Vogel, 2025), remained stable across stimulus types. Given that PI has robust effects on LTM retrieval and minimal effects on WM storage (Cowan, 2005; Oberauer et al., 2017), this selective familiarity enhancement under low-PI conditions is most parsimoniously explained by increased contributions from LTM rather than by an expansion of WM storage capacity. To summarize, when PI was equated across meaningful and simple

stimuli, memory performance was unaffected by meaningfulness, calling into question whether WM capacity is affected by meaningfulness, per se.

Experiment 2 provided converging electrophysiological evidence using the CDA. Prior studies have reported higher CDA amplitudes for meaningful than for simple stimuli and interpreted this as evidence for greater storage (Brady et al., 2016; Thibeault et al., 2024). However, most studies employed a single set size, which cannot distinguish changes in the number of items stored from load-independent differences in CDA amplitude. If meaningfulness truly increased the number of concurrently stored items, the CDA should exhibit an interaction between the stimulus type and set size, with steeper slopes and a plateau at higher set sizes for meaningful objects. Instead, CDA differences were additive across set sizes, indicating load-independent effects separable from the storage of additional items. Although CDA amplitude could be influenced by multiple cognitive operations beyond storage of discrete items, such as perceptual complexity or attentional demand (Woodman and Vogel, 2008; Drew et al., 2011; Emrich et al., 2022), the "shape" of the load function provides critical evidence regarding the number of items maintained.

Note that Experiment 2 focused on trial-unique meaningful objects and repeated colors and did not include repeated objects. Our goal was to target the condition where a meaningfulness advantage could be observed and test whether the CDA-set size function showed an interaction with the stimulus type. Because Experiment 1 demonstrated comparable behavioral capacity and recollection estimates for repeated objects and repeated colors, including the repeated objects would have added little inferential power. Thus, in the absence of any behavioral benefits, no real theoretical leverage would be achieved by measuring CDA activity for repeated objects. If the CDA was equivalent between repeated objects and colors, this would not inform storage-specific effects. If the CDA differed between repeated objects and colors, this might justify our claim that CDA activity differences can be observed in the absence of differences in WM storage (Woodman and Vogel, 2008; Drew et al., 2011) but would not clarify why trial-unique objects yielded better memory performance. Thus, CDA measurements were restricted to the more diagnostic combination of trial-unique objects and repeated colors.

From a broader theoretical perspective, these findings align with embedded-process models of WM (Cowan, 2001; Oberauer, 2002). In these frameworks, a capacity-limited focus of attention operates over activated LTM representations, maintaining a small set of individuated items in an immediately accessible state via attentional pointers that bind content to spatiotemporal context (Oberauer and Lin, 2017; Awh and Vogel, 2025). Within this architecture, meaningfulness can enhance encoding quality and decision evidence through LTM at the content level, yet the number of items concurrently maintained by attentional pointers remains limited. From this perspective, superior performance for meaningful objects under trial-unique conditions reflects enhanced contributions from LTM, without any change in active WM storage.

Classic studies indicate that WM capacity is primarily item-based. Similar capacities for single- and multifeature objects supported object-based limits (Luck and Vogel, 1997), though later work found modest costs for multifeature items but robust "object-based benefits," with features stored more effectively when bound within one object (Olson and Jiang, 2002; Hardman and Cowan, 2015; Ngiam et al., 2024). The present findings are consistent with that view. Capacity estimates converged when interference was equated, and the CDA-set size functions did not interact with the stimulus type, indicating stable item limits despite differences in stimulus richness. Similarly, associative chunking in LTM can produce apparent increases in WM performance without altering the number of concurrently maintained items. Learned word pairs or consistent color pairs can behave as single integrated items in WM tasks (Brady et al., 2009; Chen and Cowan, 2009). These benefits depend on retrievable LTM representations, rather than an expansion of WM storage (Huang and Awh, 2018; Ngiam et al., 2019). This perspective dovetails with our DPSD results, where recollection remained stable while familiarity increased under trial-unique conditions.

These results highlight PI as a critical gating mechanism that regulates interactions between episodic LTM and active WM. Under low-PI conditions, episodic LTM provides reliable, context-free familiarity signals that enhance performance (Endress and Potter, 2014). Conversely, high-PI conditions make episodic familiarity an unreliable cue to "oldness," requiring greater reliance on context-specific recollection supported by active WM bound to contextual pointers (Awh and Vogel, 2025). This gating clarifies why conventional WM paradigms using repeated stimuli yield stable capacity estimates around three or four items, whereas trial-unique paradigms can produce much inflated capacities (Endress and Potter, 2014). The inflation arises because familiarity signals from LTM boost recognition without increasing the number of WM representations. Hence, differences between trial-unique and repeated designs are not minor methodological details but determine whether behavioral performance is dominated by capacity-limited WM or shows additional contributions from LTM.

An additional consideration is semantic satiation, the temporary loss of meaning following repeated exposure, which could reduce semantic distinctiveness and impair recognition (Smith and Klein, 1990; Tian and Huber, 2010). Two observations argue against this account as the primary driver of the present findings. First, when interference was equated by repeating a fixed stimulus set, performance converged for meaningful objects and abstract colors lacking lexical-semantic associations, implicating PI rather than semantic fatigue. Second, in Experiment 2 with trial-unique objects, where satiation should be minimal, the CDA differences were additive across set sizes and showed no interaction. Satiation may exacerbate familiarity reductions for heavily repeated meaningful stimuli, but it cannot explain the full pattern of matched capacity under repetition, stable recollection, and additive CDA offsets without load interactions.

The findings connect to hierarchical views of interactions between memory systems that link perceptual and contextual binding mechanisms (Christophel et al., 2017; Yatziv and Kessler, 2018; Lee et al., 2023; Park, 2025). Perceptual memory provides large-capacity but interference-prone representations automatically encoded into activated LTM, whereas active WM engages selective binding to maintain individuated items in context. Recent neuroimaging and neurophysiological studies support this dual-code framework, with sensory-based representations sustained by posterior cortices, whereas abstract, context-bound WM states supported by frontoparietal networks (Xu and Chun, 2006; Kwak and Curtis, 2022; Chunharas et al., 2024). Intracranial recordings further dissociate medial–temporal neurons representing detailed perceptual or semantic content from frontal neurons coding abstract, slot-like WM capacities (Kamiński et al., 2017). Within this view, meaningfulness

enhances the distinctiveness of sensory representations and boosts familiarity but does not expand the number of items indexed by the attentional pointers.

Several limitations suggest promising directions. While PI was controlled through stimulus repetition, its magnitude or spatial specificity were not systematically manipulated (Lin and Luck, 2012; Makovski, 2016; Endress, 2022; Donenfeld et al., 2024). In principle, familiarity-driven gains may scale with incremental reductions of PI, and examining the temporal dynamics of PI buildup and release (Keppel and Underwood, 1962; Watkins and Watkins, 1975) could further clarify how LTM familiarity shapes performance in WM tasks. In addition, our results should be considered in light of growing research on memorability, a stimulus-intrinsic property that makes certain images consistently better remembered (Isola et al., 2013; Bainbridge, 2019), including in WM tasks (Ye et al., 2024; Tam et al., 2025). Exploring interactions between PI and memorability may elucidate how stimulus attributes and task contexts jointly influence performance, integrating stimulus-centered and process-based accounts.

In conclusion, our behavioral and neural evidence converge to show that previously reported WM capacity advantages for meaningful objects are better explained by reduced PI and elevated contributions from LTM than by expansions of WM capacity. These findings support theoretical frameworks in which a fixed-capacity attentional pointer mechanism limits the number of concurrently maintained items, while contributions from LTM are constrained by PI (Oberauer and Bartsch, 2023; Bartsch et al., 2024).

References

Adam KC, Vogel EK, Awh E (2017) Clear evidence for item limits in visual working memory. Cogn Psychol 97:79–97.

Asp IE, Störmer VS, Brady TF (2021) Greater visual working memory capacity for visually matched stimuli when they are perceived as meaningful. J Cogn Neurosci 33:902–918.

Awh E, Vogel EK (2025) Working memory needs pointers. Trends Cogn Sci 29:230–241.

Awh E, Barton B, Vogel EK (2007) Visual working memory represents a fixed number of items regardless of complexity. Psychol Sci 18:622–628.

Bainbridge WA (2019) Memorability: how what we see influences what we remember. In: *Psychology of learning and motivation*, (Ross BH, ed), Vol. 70, pp 1–27. San Diego, CA: Academic Press.

Bartsch LM, Frischkorn GT, Shepherdson P (2024) When load is low, working memory is shielded from long-term memory's influence. J Cogn 7:44.

Bays PM (2015) Spikes not slots: noise in neural populations limits working memory. Trends Cogn Sci 19:431–438.

Brady TF, Alvarez GA (2011) Hierarchical encoding in visual working memory: ensemble statistics bias memory for individual items. Psychol Sci 22: 384–392.

Brady TF, Konkle T, Alvarez GA (2009) Compression in visual working memory: using statistical regularities to form more efficient memory representations. J Exp Psychol Gen 138:487.

Brady TF, Störmer VS, Alvarez GA (2016) Working memory is not fixed-capacity: more active storage capacity for real-world objects than for simple stimuli. Proc Natl Acad Sci U S A 113:7459–7464.

Brady TF, Williams L, Störmer VS (2025) The working memory advantage for meaningful stimuli persists under high levels of proactive interference. PsyArXiv.

Brainard DH (1997) The psychophysics toolbox. Spat Vis 10:433–436.

Bunting M (2006) Proactive interference and item similarity in working memory. J Exp Psychol Learn Mem Cogn 32:183–196.

Chen Z, Cowan N (2009) Core verbal working-memory capacity: the limit in words retained without covert articulation. Q J Exp Psychol 62:1420–1429.

Christophel TB, Klink PC, Spitzer B, Roelfsema PR, Haynes JD (2017) The distributed nature of working memory. Trends Cogn Sci 21:111–124.

Chung YH, Brady TF, Störmer VS (2023) No fixed limit for storing simple visual features: realistic objects provide an efficient scaffold for holding features in mind. Psychol Sci 34:784–793.

Chung YH, Brady TF, Störmer VS (2024) Meaningfulness and familiarity expand visual working memory capacity. Curr Dir Psychol Sci 33:275–282.

Chunharas C, Wolff MJ, Hettwer MD, Rademaker RL (2024) A gradual transition toward categorical representations along the visual hierarchy during working memory, but not perception. bioRxiv.

Cowan N (2001) The magical number 4 in short-term memory: a reconsideration of mental storage capacity. Behav Brain Sci 24:87–114.

Cowan N (2005) *Working memory capacity*. New York, NY: Psychology Press.

Craig KS, Berman MG, Jonides J, Lustig C (2013) Escaping the recent past: which stimulus dimensions influence proactive interference? Mem Cognit 41:650–670.

Curby KM, Glazek K, Gauthier I (2009) A visual short-term memory advantage for objects of expertise. J Exp Psychol Hum Percept Perform 35:94–107.

Donenfeld J, Blaser E, Kaldy Z (2024) The resolution of proactive interference in a novel visual working memory task: a behavioral and pupillometric study. Atten Percept Psychophys 86:2345–2362.

Drew T, Horowitz TS, Wolfe JM, Vogel EK (2011) Delineating the neural signatures of tracking spatial position and working memory during attentive tracking. J Neurosci 31:659–668.

Emrich SM, Salahub C, Katus T (2022) Sensory delay activity: more than an electrophysiological index of working memory load. J Cogn Neurosci 35: 135–148.

Endress AD (2022) Memory and proactive interference for spatially distributed items. Mem Cognit 50:782–816.

Endress AD, Potter MC (2014) Large capacity temporary visual memory. J Exp Psychol Gen 143:548–565.

Faul F, Erdfelder E, Buchner A, Lang AG (2009) Statistical power analyses using G* power 3.1: tests for correlation and regression analyses. Behav Res Methods 41:1149–1160.

Fukuda K, Mance I, Vogel EK (2015) A power modulation and event-related slow wave provide dissociable correlates of visual working memory. J Neurosci 35:14009–14016.

Gelman A, Rubin DB (1992) Inference from iterative simulation using multiple sequences. Stat Sci 7:457–472.

Hardman KO, Cowan N (2015) Remembering complex objects in visual working memory: do capacity limits restrict objects or features? J Exp Psychol Learn Mem Cogn 41:325–347.

Huang L, Awh E (2018) Chunking in working memory via content-free labels. Sci Rep 8:1–10.

Isola P, Xiao J, Parikh D, Torralba A, Oliva A (2013) What makes a photograph memorable? IEEE Trans Pattern Anal Mach Intell 36:1469–1482.

Jonides J, Nee DE (2006) Brain mechanisms of proactive interference in working memory. Neuroscience 139:181–193.

Kamiński J, Sullivan S, Chung JM, Ross IB, Mamelak AN, Rutishauser U (2017) Persistently active neurons in human medial frontal and medial temporal lobe support working memory. Nat Neurosci 20: 590–601.

Kane MJ, Engle RW (2000) Working-memory capacity, proactive interference, and divided attention: limits on long-term memory retrieval. J Exp Psychol Learn Mem Cogn 26:336–358.

Keppel G, Underwood BJ (1962) Proactive inhibition in short-term retention of single items. J Verbal Learning Verbal Behav 1:153–161.

Kruschke JK (2015) *Doing Bayesian data analysis: a tutorial with R, JAGS, and stan*, Ed. 2. London, UK: Academic Press.

Kwak Y, Curtis CE (2022) Unveiling the abstract format of mnemonic representations. Neuron 110:1822–1828.

Lee H, Keene PA, Sweigart SC, Hutchinson JB, Kuhl BA (2023) Adding meaning to memories: how parietal cortex combines semantic content with episodic experience. J Neurosci 43:6525–6537.

Li X, Xiong Z, Theeuwes J, Wang B (2020) Visual memory benefits from prolonged encoding time regardless of stimulus type. J Exp Psychol Learn Mem Cogn 46:1998–2005.

Lin PH, Luck SJ (2012) Proactive interference does not meaningfully distort visual working memory capacity estimates in the canonical change detection task. Front Psychol 3:42.

Lopez-Calderon J, Luck SJ (2014) ERPLAB: an open-source toolbox for the analysis of event-related potentials. Front Hum Neurosci 8:213.

Luck SJ, Vogel EK (1997) The capacity of visual working memory for features and conjunctions. Nature 390:279–281.

Luria R, Balaban H, Awh E, Vogel EK (2016) The contralateral delay activity as a neural measure of visual working memory. Neurosci Biobehav Rev 62:100–108.
Makovski T (2016) Does proactive interference play a significant role in visual working memory tasks? J Exp Psychol Learn Mem Cogn 42:1664–1672.
Ngiam WX, Brissenden JA, Awh E (2019) "Memory compression" effects in visual working memory are contingent on explicit long-term memory. J Exp Psychol Gen 148:1373–1385.
Ngiam WX, Foster JJ, Adam KC, Awh E (2023) Distinguishing guesses from fuzzy memories: further evidence for item limits in visual working memory. Atten Percept Psychophys 85:1695–1709.
Ngiam WX, Loetscher KB, Awh E (2024) Object-based encoding constrains storage in visual working memory. J Exp Psychol Gen 153:86.
Oberauer K (2002) Access to information in working memory: exploring the focus of attention. J Exp Psychol Learn Mem Cogn 28:411.
Oberauer K, Bartsch LM (2023) When does episodic memory contribute to performance in tests of working memory? J Cogn 6:44.
Oberauer K, Lin HY (2017) An interference model of visual working memory. Psychol Rev 124:21.
Oberauer K, Awh E, Sutterer DW (2017) The role of long-term memory in a test of visual working memory: proactive facilitation but no proactive interference. J Exp Psychol Learn Mem Cogn 43:1–22.
Olson IR, Jiang Y (2002) Is visual short-term memory object based? Rejection of the "strong-object" hypothesis. Percept Psychophys 64:1055–1067.
Park HB (2025) Contextual pointers and sensory codes in working memory: Toward a hierarchical framework. PsyArXiv.
Park HB, Zhang W (2024) The dynamics of attentional guidance by working memory contents. Cognition 242:105638.
Park HB, et al. (2023) Contributions of global and local processing on medical image perception. J Med Imaging 10:S11911.
Quirk C, Adam KC, Vogel EK (2020) No evidence for an object working memory capacity benefit with extended viewing time. eNeuro 7:5.
Schurgin MW, Wixted JT, Brady TF (2020) Psychophysical scaling reveals a unified theory of visual memory strength. Nat Hum Behav 4:1156–1172.
Shoval R, Gronau N, Sidi Y, Makovski T (2023) Objects' perceived meaningfulness predicts both subjective memorability judgments and actual memory performance. Vis cogn 31:472–484.
Smith L, Klein R (1990) Evidence for semantic satiation: repeating a category slows subsequent semantic processing. J Exp Psychol Learn Mem Cogn 16:852.
Standing L (1973) Learning 10000 pictures. Q J Exp Psychol 25:207–222.
Tam J, Green T, O'Donnell RE, Wyble B (2025) Memorability effects emerge in incidental visual working memory. J Exp Psychol Learn Mem Cogn 51: 1376–1391.
Thibeault AM, Stojanoski B, Emrich SM (2024) Investigating the effects of perceptual complexity versus conceptual meaning on the object benefit in visual working memory. Cogn Affect Behav Neurosci 24:453–468.
Tian X, Huber DE (2010) Testing an associative account of semantic satiation. Cogn Psychol 60:267–290.
Torres RE, Duprey MS, Campbell KL, Emrich SM (2025) Not all objects are created equal: the object benefit in visual working memory is supported by greater recollection-like memory, but only for memorable objects. Mem Cognit 53:1343–1355.
van den Berg R, Awh E, Ma WJ (2014) Factorial comparison of working memory models. Psychol Rev 121:124.
Vogel EK, Machizawa MG (2004) Neural activity predicts individual differences in visual working memory capacity. Nature 428:748–751.
Watkins OC, Watkins MJ (1975) Buildup of proactive inhibition as a cue-overload effect. J Exp Psychol Hum Learn Mem 1:442.
Woodman GF, Vogel EK (2008) Selective storage and maintenance of an object's features in visual working memory. Psychon Bull Rev 15: 223–229.
Xu Y, Chun MM (2006) Dissociable neural mechanisms supporting visual short-term memory for objects. Nature 440:91–95.
Yatziv T, Kessler Y (2018) A two-level hierarchical framework of visual short-term memory. J Vis 18:2–2.
Ye C, Guo L, Wang N, Liu Q, Xie W (2024) Perceptual encoding benefit of visual memorability on visual memory formation. Cognition 248:105810.
Yonelinas AP (2002) The nature of recollection and familiarity: a review of 30 years of research. J Mem Lang 46:441–517.
Yonelinas AP, Aly M, Wang WC, Koen JD (2010) Recollection and familiarity: examining controversial assumptions and new directions. Hippocampus 20:1178–1194.
Yonelinas AP (2024) The role of recollection and familiarity in visual working memory: a mixture of threshold and signal detection processes. Psychol Rev 131:321–348.
Zhao C, Vogel E, Awh E (2023) Change localization: a highly reliable and sensitive measure of capacity in visual working memory. Atten Percept Psychophys 85:1681–1694.